

Numerical and experimental investigation of mechanical stress in the processing of chunky fruit preparations

L Vulprecht*, T Wölken, C Rauh

Technische Universität Berlin, Department of Food Biotechnology
and Food Process Engineering, Berlin, Germany

*lennart.vulprecht@tu-berlin.de

Abstract

The transport of particle dispersions in a fluid matrix plays an important role in natural and technological processes. Within such transport processes, the accumulation as well as physicochemical and biological transformations of the dispersion might take place simultaneously and thus detailed knowledge of the fluid mechanics within the dispersion is of high interest in food and other processing technologies. Information about these mechanics can be obtained using optical measurement techniques such as Laser Doppler Anemometry (LDA), Particle Tracking Velocimetry (PTV) and Particle Image Velocimetry (PIV). However, applications of these techniques in fluid mechanics research are limited by several factors. The systems need to be transparent to some extent and refraction by the materials involved can cause problems regarding both the sufficient illumination of the flow and the reliability of the signal. This is especially true for the investigation of multi-phase flows where refracting interfaces may be present anywhere in the control volume and are also mobile. Model systems are often developed to grant optical access while still behaving in a way similar to the original system. One way to ensure reliability of the results is to match the refractive indices of all relevant components in the experimental setup. Highly concentrated dispersions have not been researched extensively due to the strong limitations set by the difficult environment of such phenomena, be it for invasive or non-invasive diagnosis methods. Due to material properties such as plasticity, elasticity and rheological behavior of the fluid, the solid phase cannot be investigated with invasive measurement methods because the sensor will interact with the dispersion and hence the results will not be precise. The context of the presented research is the fluid mechanical analysis of stirred chunky fruit preparations, where solid matter particles are present that are vulnerable to mechanical influences. Fruit preparations are typically highly loaded with particles and have a high variety of available interactions. To investigate specific mechanical interactions with the fluid, with the apparatus and of the particles with each other, a stirring tank setup is created where all relevant components are transparent with matching refractive indices.

1 Introduction

This research is aimed at the optimization of mixing processes regarding mechanical stress in the processing of chunky fruit preparations. Simulation models are developed to create artificial neural networks capable of predicting optimal process parameters for individual stirring setups depending on

specific product and process requirements. Velocity and stress distributions are derived in fluid mechanical experiments to validate these numerical models. The strategy is thus neuro-numerical and based mainly on Particle Image/Tracking Velocimetry (PIV/PTV), Computational Fluid Dynamics (CFD), and machine learning. Chunky fruit preparations are very complex systems which can be described best (if at all) using hybrid methods extending the possibilities of conventional fluid CFD (Díez Robles, 2009). Particle-laden turbulent flows have been researched extensively (e.g. Elghobashi, 2006) due to their importance across many process engineering disciplines. A useful introduction into the basic and advanced theory of stirring flows is provided by the *Mixing* chapter in *Food Process Engineering and Technology* (Berk, 2013), while the necessary basics for optical measurement (PIV and PTV) are compiled in the very comprehensive *Particle Image Velocimetry: A Practical Guide* (Raffel, et al., 2007).

2 Experiments

2.1 Refractive Index Matching (RIM)

Refractive differences are a significant challenge when measuring flow situations with two or more phases and multiple interfaces moving around in the observed volume. Refractive index matching has been documented for several setups (Bai & Katz, 2014; Budwig, 1994; Byron & Variano, 2013; Cui & Adrian, 1994; Daviero, et al., 2001; Franklin & Wang, 2002). In these cases, liquid and solid components used in the experiment consist of materials selected to refract light equally or similarly within an accepted range. However, most transparent solid materials have refractive indices of 1.5 and above while most available liquids have significantly lower indices, e.g. water: 1.33 (Polyanskiy, 2017).

2.2 Materials

Transparent PMMA (Plexiglas), with a particularly low refractive index of 1.49, is chosen here as the material for the apparatus. Highly concentrated aqueous sodium iodide solution (64%w/w NaI) with an index of 1.49 is used as the liquid medium in a first stage. In a second stage, NaI is combined with sucrose in order to change the viscosity of the medium while keeping the refractive index constant. Particles are made by solidifying the solution using hydrocolloids. First attempts to produce gels mimicking the mechanical properties of fruit matter used κ -carrageenan because of its excellent gelling properties as described in the literature (Belitz, et al., 2008; Campo, et al., 2009; Rochas, 1984) but at a high concentration of sodium iodide, the gels turn out to be significantly weaker. Combinations with other hydrocolloids were tested. For most hydrocolloids, a high concentration of salt (NaI) severely impedes their solidification; in addition, a high concentration of iodide ions often causes dark discoloration similar to a starch-iodine reaction. After many attempts, combination of locust bean gum with κ -carrageenan proved successful. The stirrer made from PMMA is of a modified anchor type operated in a stirring vessel with a torispherical bottom as depicted in Figure 1. A similar apparatus is used in the industry for particle-laden liquids such as fruit juices with pulp content to ensure an even distribution of solids.

2.3 Setup and Parameters

Aqueous NaI solution (64 %w/w) with a density of 1850 kg/m³ and a Newtonian viscosity measured to be 3,5 mPas at room temperature is stirred in an apparatus as depicted in Figure 1. The rotational speed of $n=40$ rpm corresponds, with the given parameters of this setting, to a Reynolds number of about 4110. PMMA particles with a mean diameter of $d=50$ μm are used as tracers. The stirred volume is illuminated

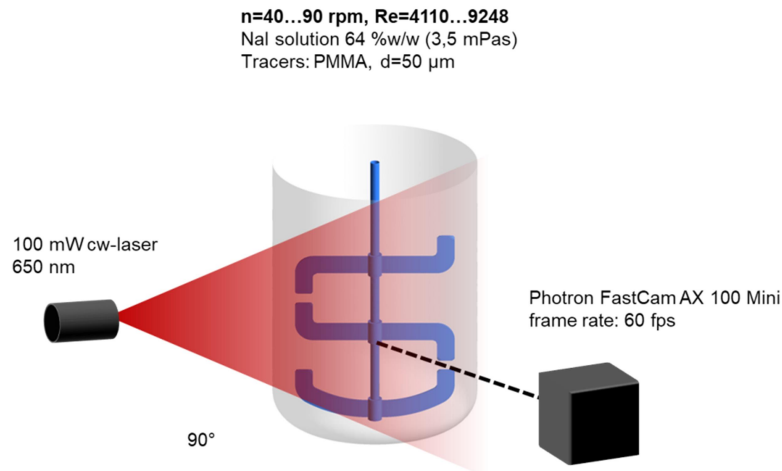


Figure 1: Setup of stirring experiments with PIV system

with a 100 mW laser line module (continuous wave) at a wavelength of 650 nm in the central vertical plane of the vessel. Images are taken with a Photron FastCam AX 100 Mini camera at a frame rate of 60 fps. In single-phase stirring experiments, only 64%w/w sodium iodide solution is stirred. In the two-phase-stage, gel particles are added made with 0.2% locust bean gum and 0.2% κ -carrageenan. The gels were cast and then passed through a sieve of 2 mm mesh width to obtain a particle diameter distribution around a 2 mm average. The particle volume fraction was varied from about 10% to about 50% in steps of 10%. The rotational speed was varied between 30 rpm and 90 rpm in steps of 10 rpm.

3 Simulation

Simulating a suspension flow of macroscopic particles poses a great challenge, because established approaches in two-phase CFD modelling do not sufficiently represent the properties of their mechanics. The Euler-Lagrange approach traditionally represents the particles as point masses and is therefore only applicable for low volume fractions of the particulate phase. This is obviously unfit for flow situations with particle volume fractions of up to 50% and a size range around several millimeters, where particles are bound to collide with each other. The Euler-Euler approach does not take into account individual particles and treats both phases as interpenetrating continua. Like the Euler-Lagrange approach, it was not developed with the intention of simulating particles that exceed the cell size of the domain discretization. Particle collisions are not directly simulated and have to be taken into account with additional and often inaccurate models. Such simulations can only provide part of the mechanical information required.

These conventional simulation models do not satisfy the requirements of the given investigation. A hybrid approach is used that solves the flow field with a conventional Euler-Euler CFD simulation and simultaneously uses discrete element modelling to compute particle-particle and particle-geometry collisions to obtain mechanical forces. The results of both simulations are then coupled to exchange fluid-particle interactions. A 2300 liter tank is modelled as containing particles of 0.6 cm diameter with a volume fraction of 1%. The stirring flow is characterized with a Reynolds number of 44600. The flow creates a clear area of particle depletion through collisions as well as a spiraling (cyclonic) flow pattern. The ratio of grid size and particle diameter is a limiting factor in this setup and expanding it to larger particles is problematic. However, results can be used as a basis to extend the Euler-Euler simulation. As shown in Figure 2, the depletion of particles computed with conventional CFD alone does not match with

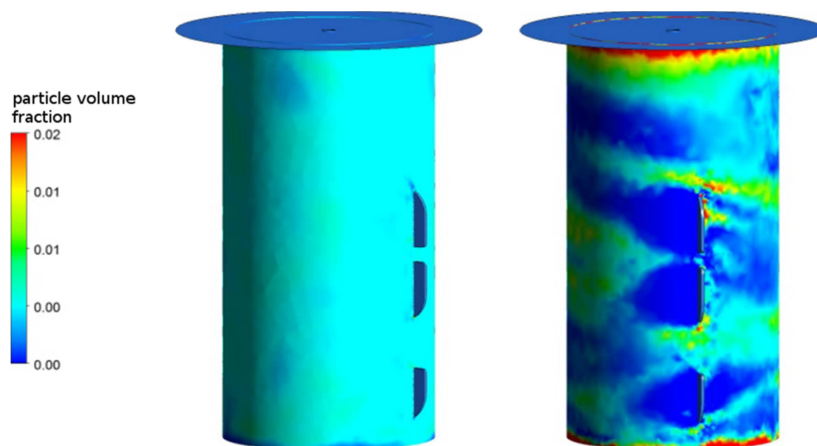


Figure 2: Particle distribution patterns predicted by classic CFD (left) and CFD-DEM coupling (right) for the same suspension after 4 seconds of simulated stirring time.

that of CFD-DEM coupling. This coupling approach can be used to gather insight, such as the location of collisions and the distribution of collision forces. Generally, it is also of interest which flow parameters characterize collisions most reliably. The answers will be used to extend the Euler-Euler equation with a momentum equation for multiphase simulations. Apparently, collisions are concentrated at the same locations where velocity gradients are large. The spatial distribution of collision forces also shows that the strongest events (with the most potential for detrimental effects) happen in the wake of the agitating arms. Shear rate values are highest at the edges of the stirrer and the positions of the most forceful collisions match the areas of high shear (high velocity gradients in the flow field lead to collisions).

4 Results

In single-phase stirring experiments, a good match between measured and simulated velocity distributions results has been observed with velocity magnitudes in both distributions ranging from 0 to 65 mm/s. Figure 3 illustrates that in a two-phase experiment the absolute velocities are still in the same order of magnitude. A combination of increased particle loading and more revolutions per minute leads to significantly higher velocity magnitudes, while more particles or faster stirring alone had no pronounced effect. First CFD-DEM simulation runs imply that position and force value of collisions and even the volume fraction distribution can in fact be correlated with flow parameters such as dynamic pressure and velocity gradients. The next step will be the extension of the momentum equation by a corrective function $\eta(p,u)$ to modify the drag included in the phase coupling term and enabling the prediction of collisions. This will ultimately complete the modified Euler-Euler simulated model of a chunky fruit preparation.

5 Prospect

Further series of experiments will focus on variation of the rheology, preferably by introduction of a non-Newtonian RIM liquid. First trials show that sodium iodide and sucrose may interact to create a shear-thinning effect in a mutual solution. Extending the applicability of the simulation model to geometry interactions and collisions must involve either additional source terms or CFD-DEM-coupling. If this is not feasible, partitioning in size ranges and computing as one phase per range might be a useful alternative (population balance approach); in that case, transition flows between size ranges would be calculated according to stress load history. Shear, strain and collision have to be considered and accounted for in a

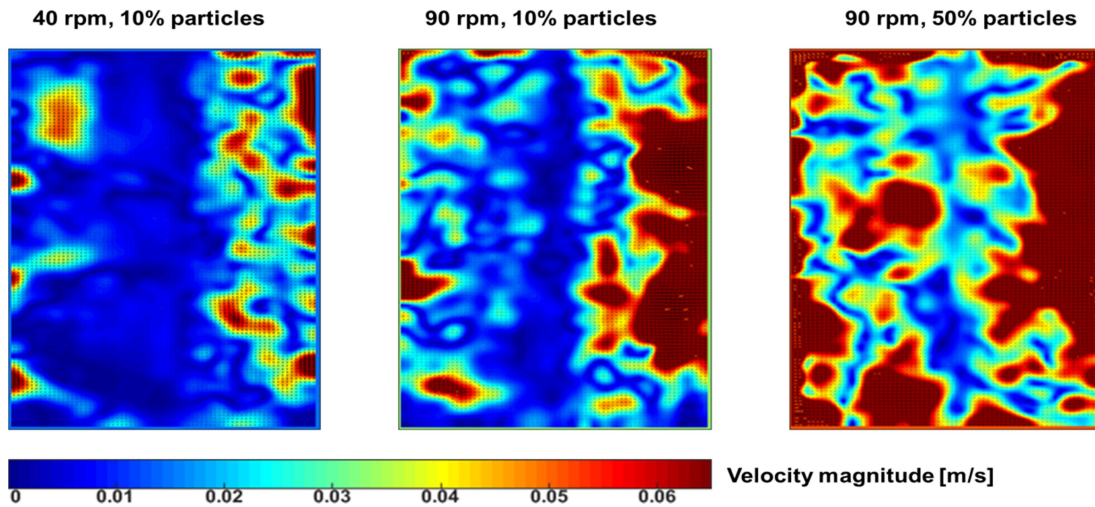


Figure 3: Velocity distributions for three different parameter combinations

bulk value parameter that is yet to be defined. Results could then also be validated with conventional sifting analysis as well as particle image analysis.

Acknowledgements

This research is made possible as an IGF project of the AiF (project number AiF 19011N) funded by Forschungskreis der Ernährungsindustrie e. V. (FEI) Bonn in cooperation with the German Institute of Food Technology (DIL).

References

- ANSYS, 2015. *Fluent 16 Theory Guide*. s.l.:ANSYS Inc..
- Bai, K. & Katz, J., 2014. On the refractive index of sodium iodide solutions for index matching in PIV. *Experiments in Fluids (Vol 55)*, p. 1704 ff..
- Belitz, H.-D., Grosch, W. & Schieberle, P., 2008. *Lehrbuch der Lebensmittelchemie*. Berlin Heidelberg: Springer Verlag.
- Berk, Z., 2013. Chapter 7 - Mixing, In Food Science and Technology. In: *Food Process Engineering and Technology (Second Edition)*. San Diego: Academic Press, pp. 193-216.
- Budwig, R., 1994. Refractive index matching methods for liquid flow investigations. *Experiments in Fluids (Vol 17)*, pp. 350-355.
- Byron, M. L. & Variano, E. A., 2013. Refractive-index-matched hydrogel materials for measuring flow-structure interactions. *Experiments in Fluids (Vol. 54)*, p. 1456ff..
- Campo, V. L., KaWano, D. F., da Silva J., D. B. & Carvalho, I., 2009. Carrageenans: biological properties, chemical modifications and structural analysis - a review. *Carbohydrate Polymers (Vol 77)*, pp. 167-180.

5th International Conference on Experimental Fluid Mechanics – ICEFM 2018 Munich
Munich, Germany, July 2-4, 2018

- Cui, M. M. & Adrian, R. J., 1994. Refractive index matching and marking methods for highly concentrated solid-liquid flows. *Experiments in Fluids (Vol 22)*, pp. 261-264.
- Daviero, G., Roberts, P. J. & Maile, K., 2001. Refractive index matching in large-scale stratified experiments. *Experiments in Fluids (Vol 31)*, pp. 119-126.
- Díez Robles, L., 2009. *Novel Hybrid Methods Applied for the Numerical Simulation of Three-Phase Biotechnological Flows*. Erlangen: Universität Erlangen-Nürnberg.
- Elghobashi, S., 2006. *An Updated Classification Map of of Particle-Laden Turbulent Flows*. Dordrecht, Springer.
- Franklin, J. & Wang, Z. Y., 2002. Refractive Index Matching: A General Method for Enhancing the Optical Clarity of a Hydrogel Matrix. *Chemistry of Materials (Vol. 14)*, pp. 4487-4489.
- Kraft, A.-L., 2012. *Charakterisierung der Beanspruchungsmechanismen scherempfindlicher Stoffsysteme im Rührprozess*. Neubrandenburg: Hochschule Neubrandenburg.
- MATLAB, 2016. *MATLAB and Image Processing Toolbox Release 2016b*. Natick, Massachusetts, USA: The Mathworks Inc..
- Moreira, L. .. S. & Filho, E. X. F., 2008. An overview of mannan structure and mannan-degrading enzyme systems. *Applied Microbiology and Biotechnology (Vol 79)*, pp. 165-178.
- Polyanskiy, M., 2017. *Refractive Index Info*. <https://refractiveindex.info/>: last accessed 15/05/2017.
- Raffel, M., Willert, C. E., Wereley, S. & Kompenhans, J., 2007. *Particle Image Velocimetry: A Practical Guide*. Berlin Heidelberg: Springer-Verlag.
- Rochas, C. R. M., 1984. Mechanism of gel formation in k-Carrageenan. *Biopolymers (Vol 23)*, pp. 735-745.
- Thielicke, W. & Stamhuis, E. J., 2016. *PIVlab - Time-Resolved Digital Particle Image Velocimetry Tool for MATLAB*. Latest version v1.4: s.n.
- Wiederseiner, S., Andreini, N., Epely-Chauvin & G., A. C., 2011. Refractive-index and density matching in concentrated particle suspensions: a review. *Experiments in Fluids (Vol 50)*, pp. 1183-1206.
- Yu, G. et al., 2002. Structural studies on k-Carrageenan derived oligosaccharides. *Carbohydrate Research (Vol 337)*, pp. 433-440.
- Zima-Kulisiewicz, B., 2008. *Einfluss von fluiddynamischen Effekten auf granularen Belebtschlamm*. Erlangen: Dissertation, Universität Erlangen-Nürnberg.